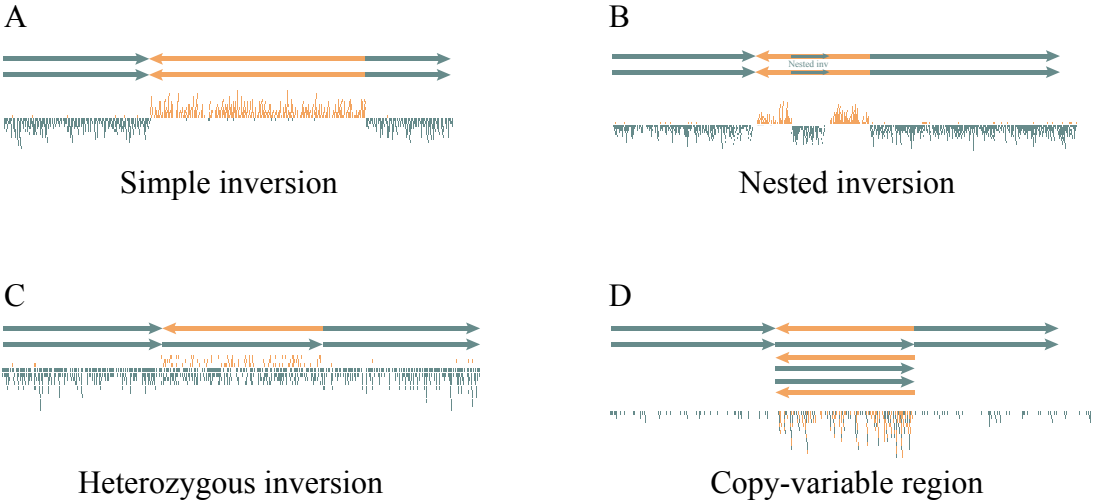

Supplemental Fig. S1. Strand-seq schematic view of the different rearrangements. A. Simple inversions appear as segmental changes in strand orientation along a chromosome with a complete switch in reads directionality (green to orange) when in homozygous state. Green reads mapping within the orange ones represent libraries background. Different classes of background can be identified in Strand-seq libraries as previously described by Sanders and colleagues (Sanders 2017). **B.** Nested inversions map within a larger inversion, thus appear direct by Strand-seq. **C.** Heterozygous inversions show a partial switch in reads directionality resulting in a mix of green and orange reads. **D.** Copy-variable regions show an increased read depth of the region and result in a mix of orange and green reads.

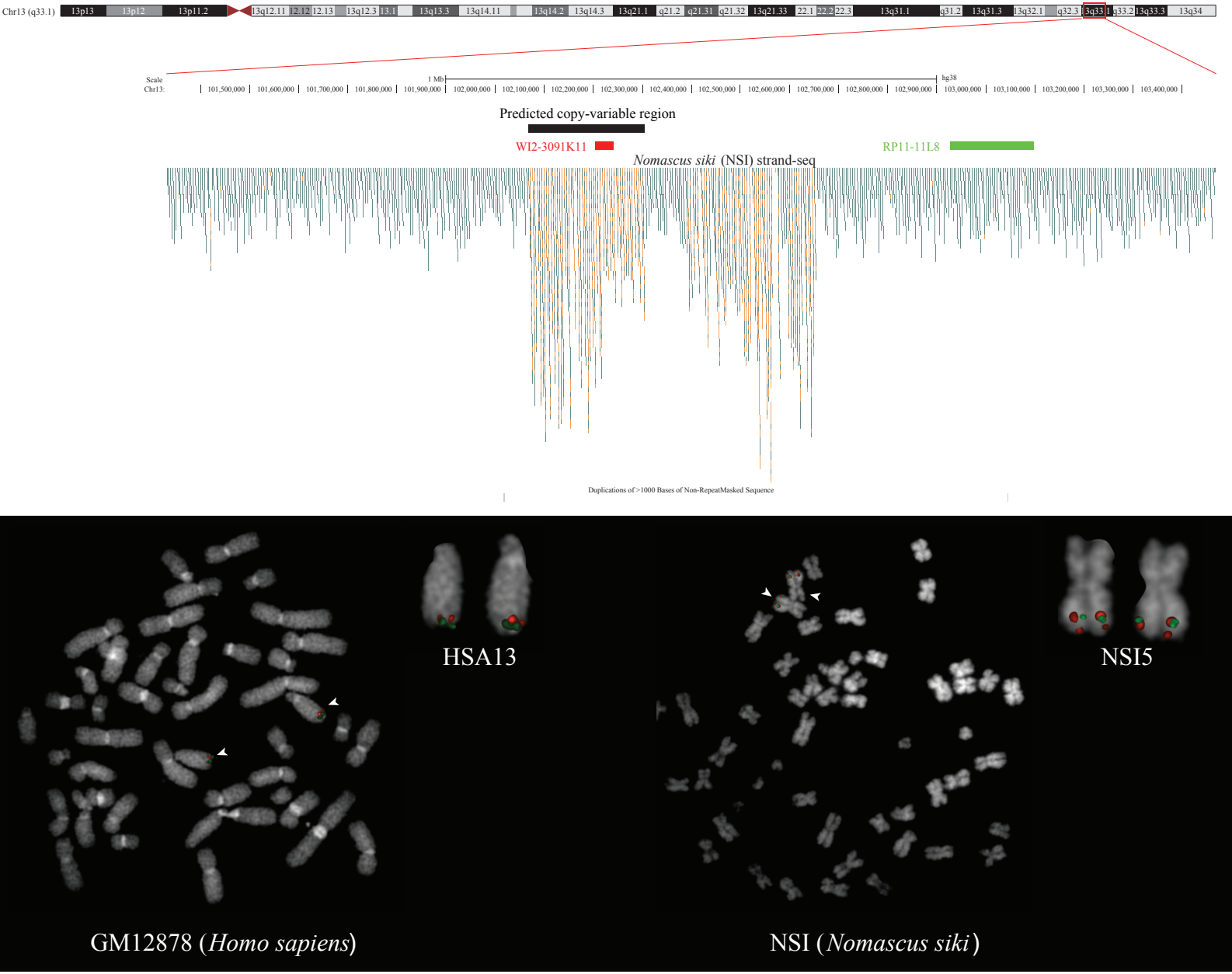

Supplemental Fig. S2. FISH validation of a copy-variable region. The top panel shows the UCSC Genome Browser view of the 13q33.1 region, the predicted copy-variable region (black bar), and the two probes used for the FISH experiments (red clone internal to the region, green control clone within a single copy region). Bottom, the red probe shows a single signal on both Chromosome 13 homologues in a human metaphase and a duplicated signal in *Nomascus*, while the green control probe is single copy in both species.

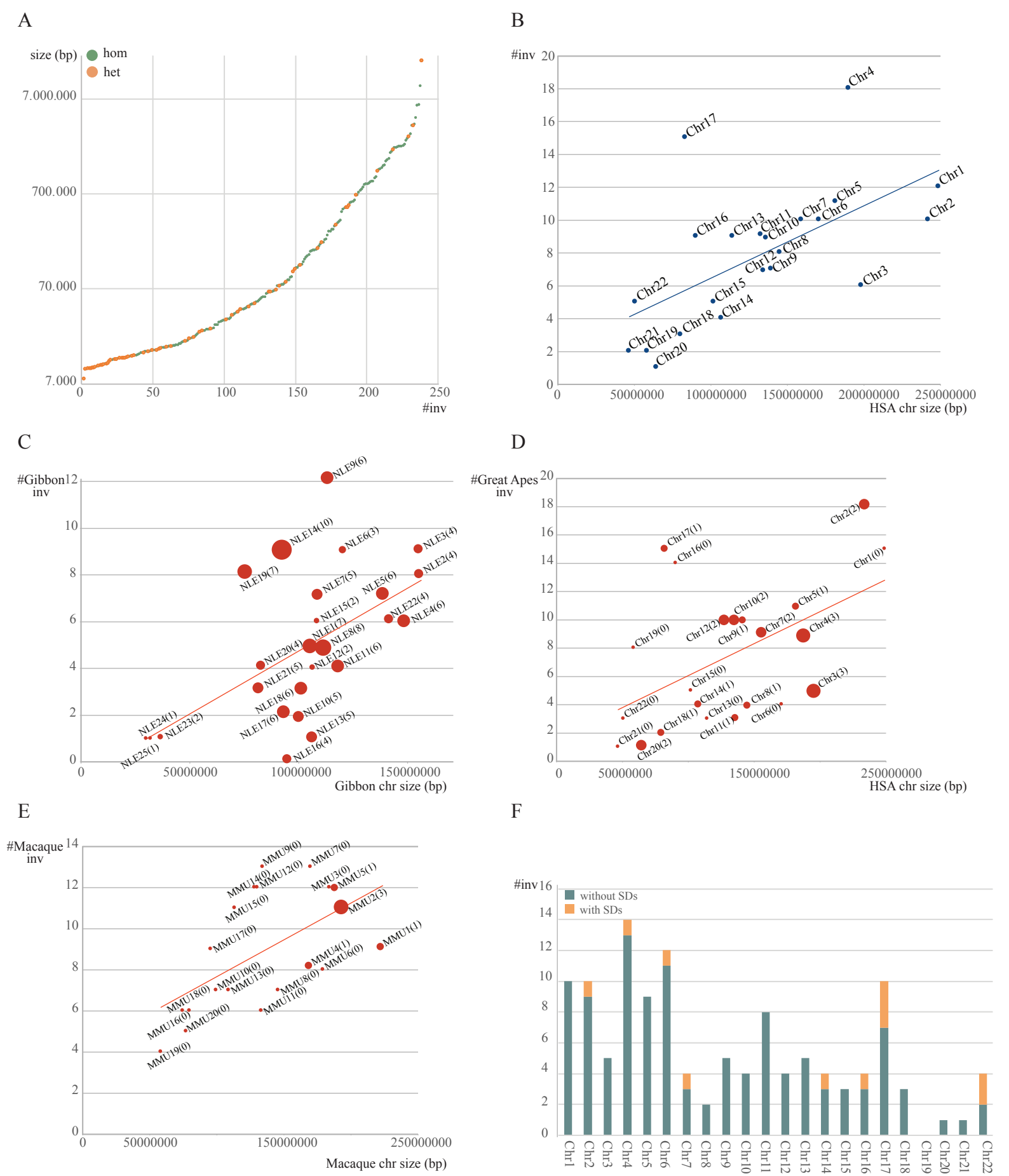

Supplemental Fig. S3. Size and distribution of inversions. A. The image shows the number of inversions detected by Strand-seq (x-axis) and their size (y-axis). Green dots represent inversions in homozygous state while orange dots represent those in heterozygous state. **B.** The image shows the number of inversions detected by Strand-seq (y-axis) for each human chromosome with respect to the size of human chromosomes (x-axis). **C.** The number of gibbon-specific inversions (y-axis) for each chromosome with respect to the size of gibbon chromosomes (x-axis) is shown. The size of the red circles is proportional to the number of gibbon large scale chromosome rearrangements (shown in parenthesis) (http://www.biologia.uniba.it/gibbon/chromosomes/Fig_3_NLE_synteny.html) (Carbone et al. 2014). **D.** The number of great apes inversions (y-axis) for each chromosome with respect to the size of human chromosomes (x-axis) is shown. The size of the red circles is proportional to the number of great apes large scale chromosome rearrangements (shown in parenthesis). **E.** The number of macaque inversions (y-axis) for each chromosome with respect to the size of human chromosomes (x-axis) is shown. The size of the red circles is proportional to the number of macaque large scale chromosome rearrangements (shown in parenthesis). **F.** The image shows the number of gibbon-specific inversions detected by Strand-seq (y-axis) for each chromosome and the presence or absence of SDs at both BPs.

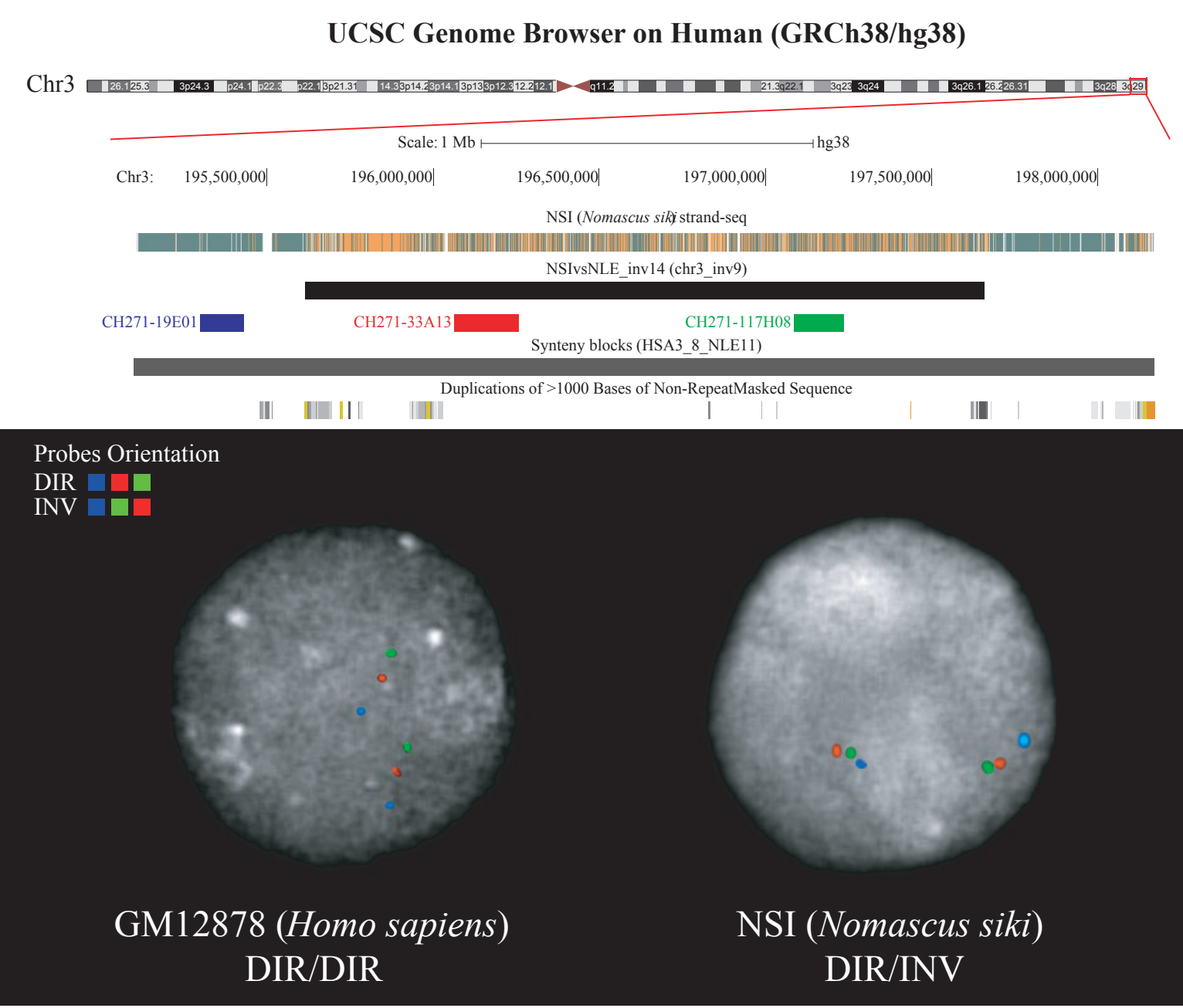

Supplemental Fig. S4. FISH analysis of the polymorphic inversion (Chr3_inv9) in NSI. NSI Strand-seq view of HSA Cchromosome 3, shows the incomplete switch in the orientation of a 2-Mbp region, suggesting the presence of a heterozygous inversion (chr3_inv9) against the human (hg38) reference genome. The region was tested using FISH in interphase nuclei in human and NSI. The inversion is present in NSI proving the heterozygous state shown by the Strand-seq data. (HSA) *Homo sapiens*; (NSI) *Nomascus siki*.

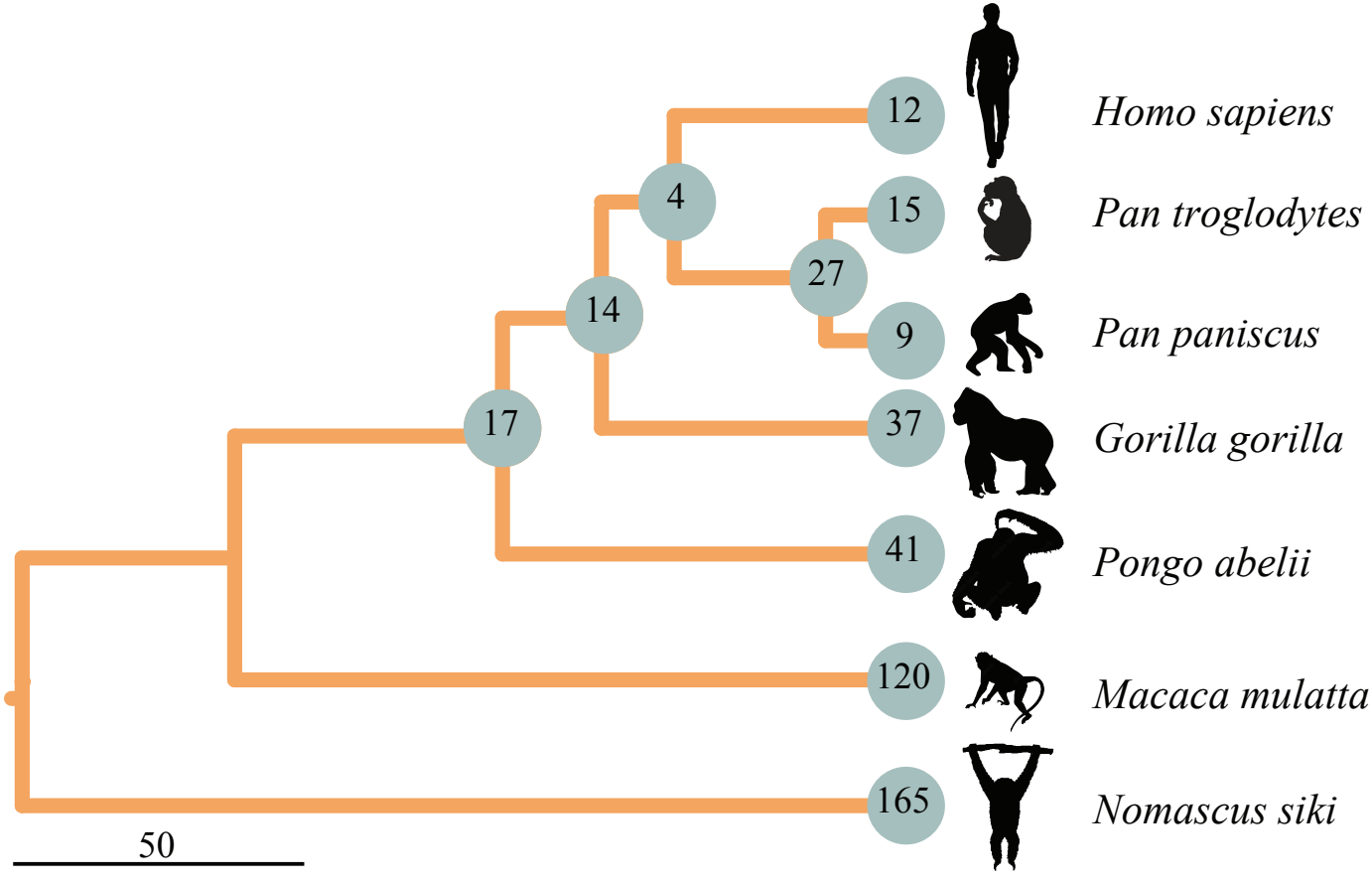

Supplemental Fig. S5. Hierarchical clustering tree of 536 inversions. Hierarchical clustering tree based on a Manhattan distance matrix constructed taking into consideration presence or absence of in 536 inversions. The scale refers to the distance in number of inversion loci. Numbers on nodes refer to shared inversion presence on the underlying subtrees, while numbers on branches refer to private number inversions. Note that the topology of the tree is inconsistent with the evolutionary tree in Figure 3A, given to the high number of private inversions in *Nomascus leucogenys*.

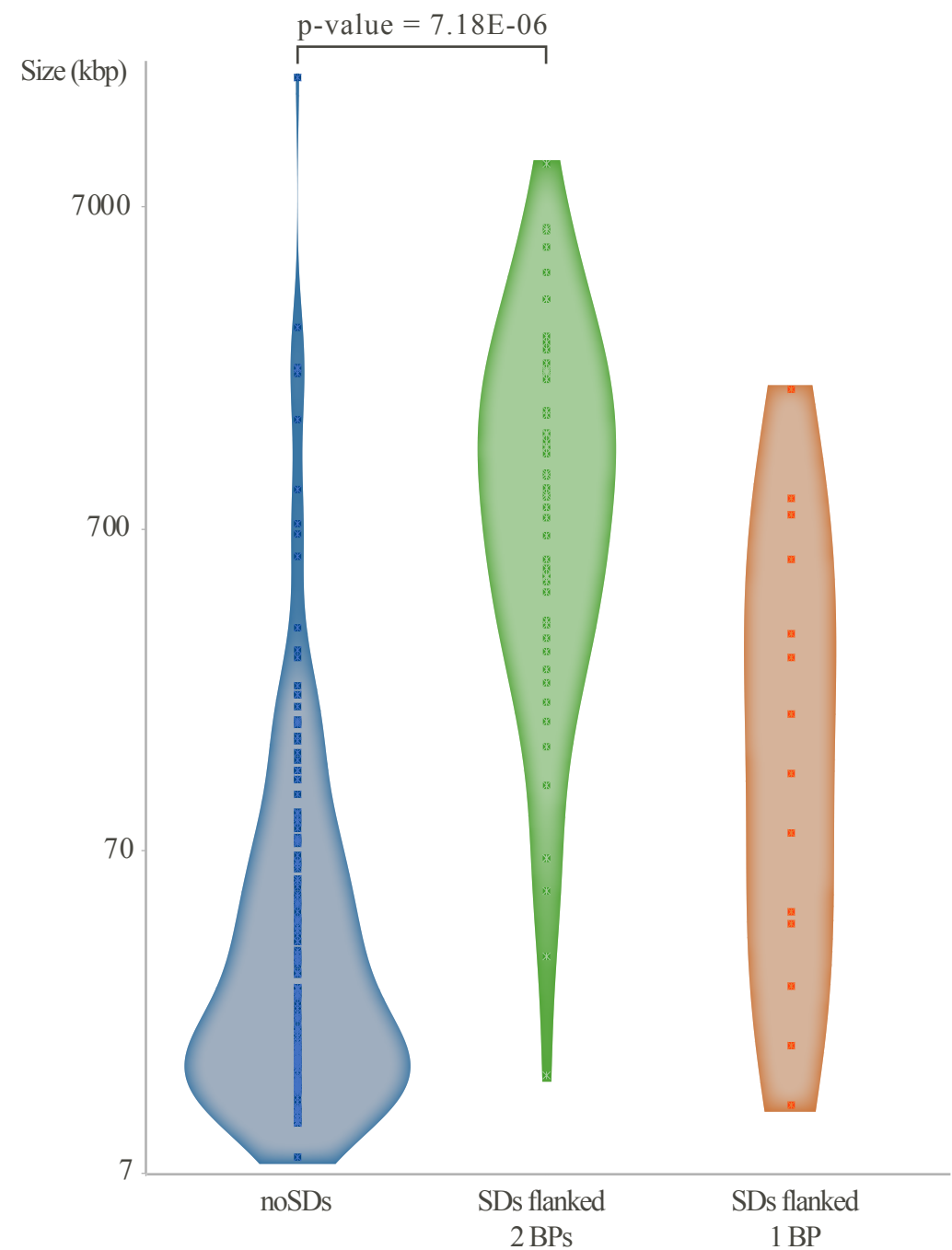

Supplemental Fig. S6. Violin plot of inversions' sizes. The inversions are clustered by the presence of SDs at their BPs. In blue, no SDs; in green, SDs mapping at both BPs; in red, SDs mapping at one inversion BP.

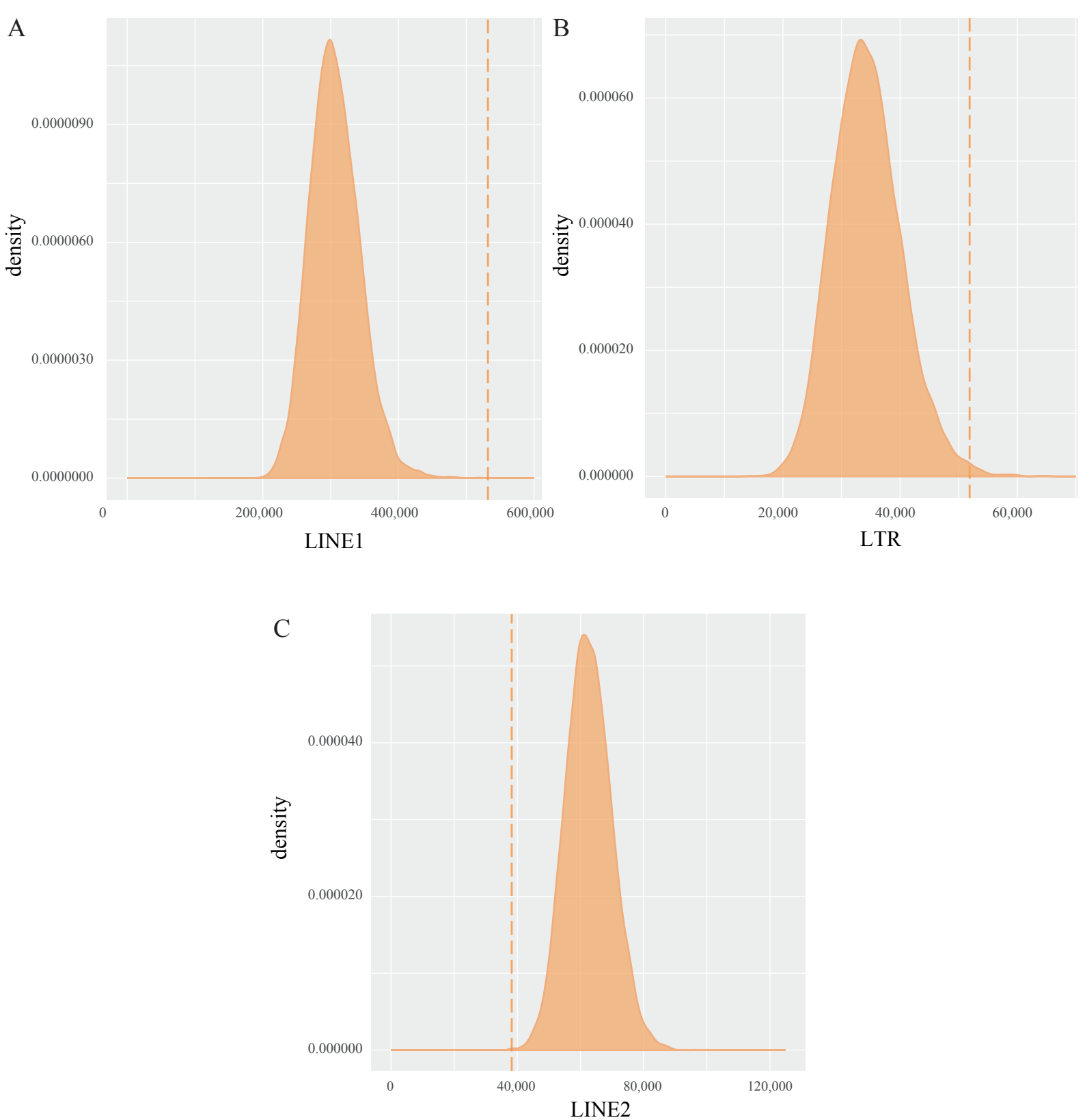

Supplemental Fig. S7. Repeat content at inversion breakpoints. The figure shows data comparisons between 10,000 random clusters of shuffled (orange area) and gibbon-specific BP regions without SDs (dashed line) in human GRCh38 for LINE1 (panel A) and LTR (panel B) (both enriched in the BP regions), and LINE2 (panel C) (as an example of repeat class depletion in the BP regions).

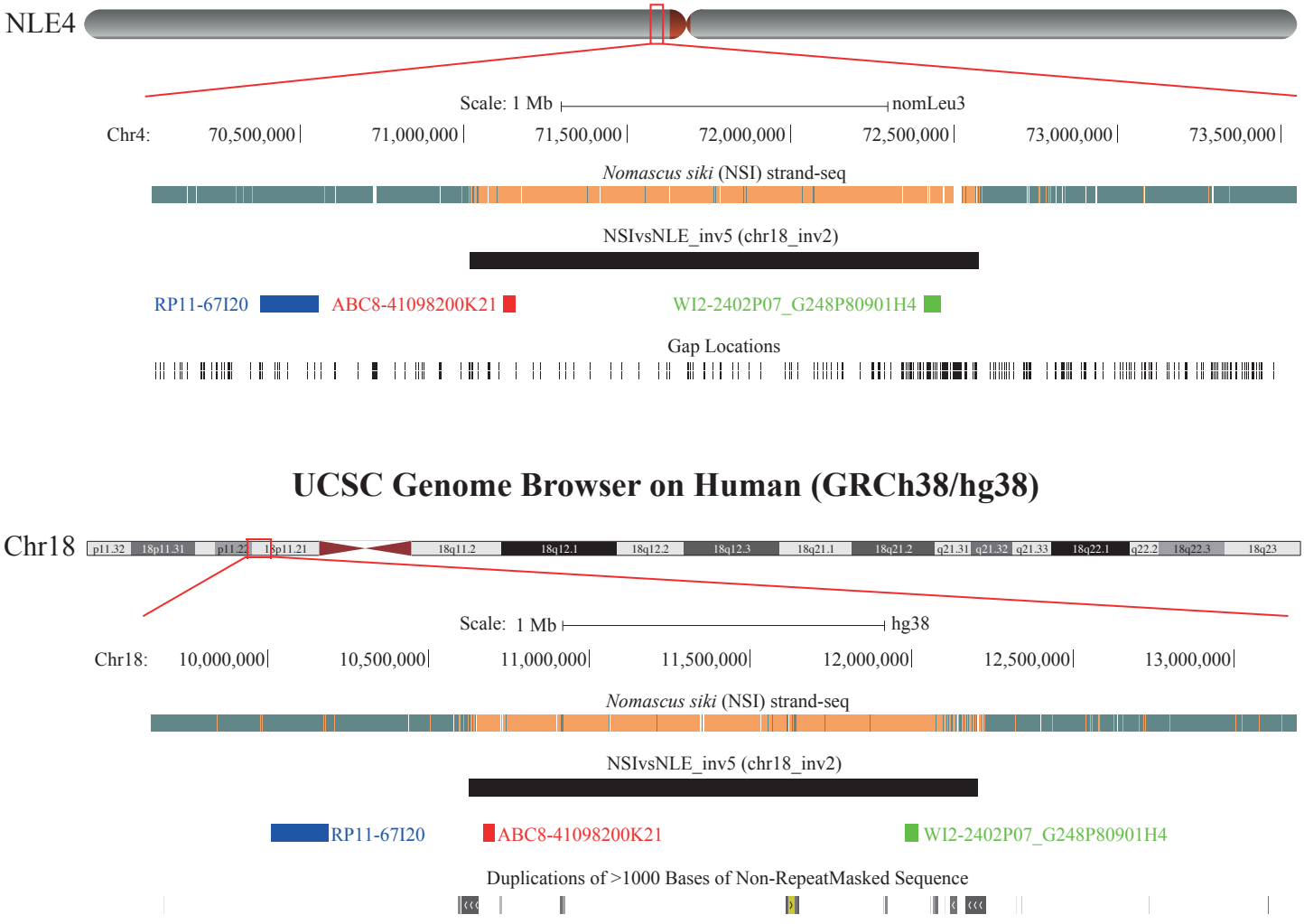

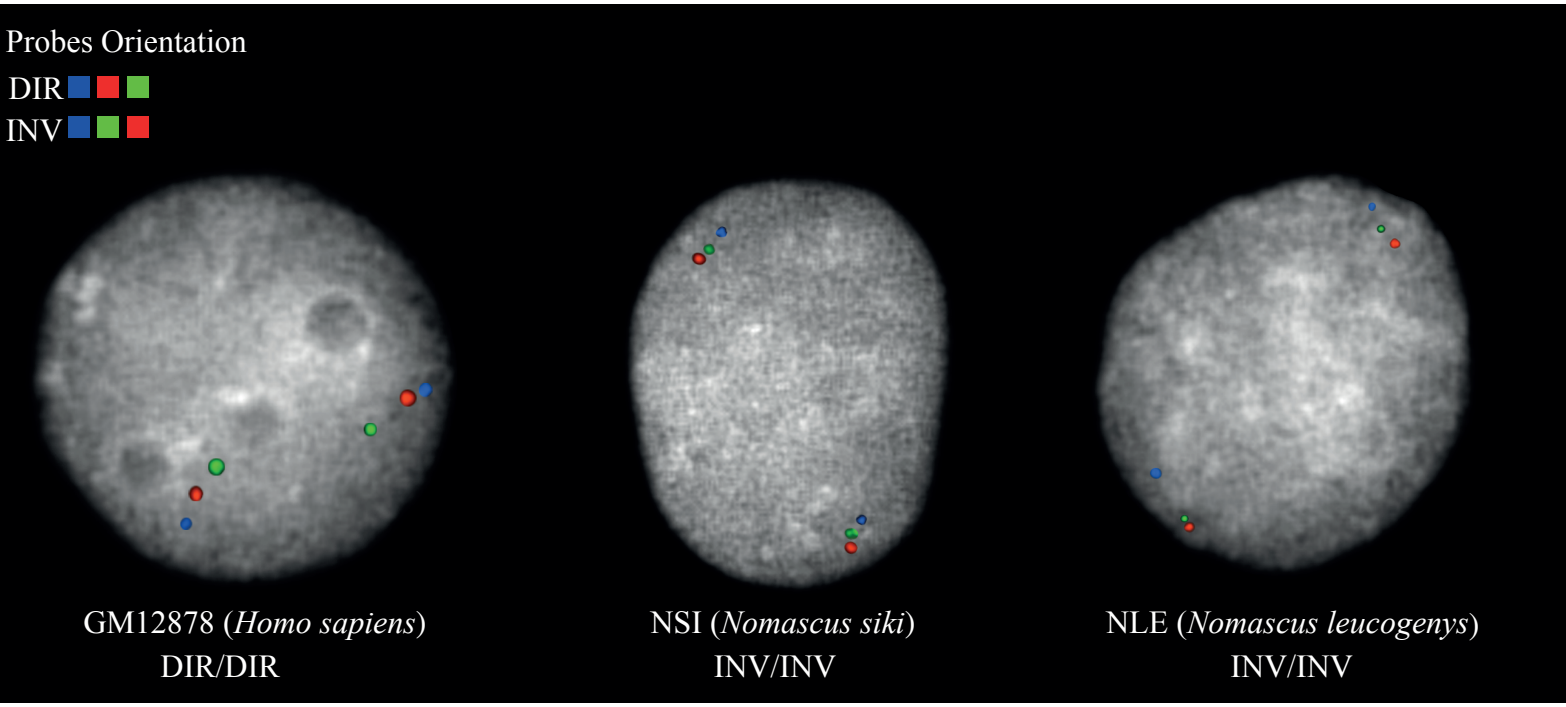

Supplemental Fig. S8. FISH analysis of chr18_inv2 inversion reveals a misassembly in the gibbon GGSC Nleu3.0/nomLeu3 reference. NSI Strand-seq view of NLE Cchromosome 4 and HSA Cchromosome 18, shows the switch in the orientation of a 1.5-Mbp region, suggesting the presence of an inversion (chr18_inv2) against both gibbon (Nleu3) and human (hg38) reference genomes. The region was tested using FISH in interphase nuclei in human and two species of gibbon, NSI and NLE. The region is in the same orientation in both gibbon species proving the misassemblies of the gibbon reference. (HSA) *Homo sapiens*; (NSI) *Nomascus siki*; (NLE) *Nomascus leucogenys*.